Linear and Nonlinear Control of a Three Pole Combined Active Magnetic Bearing - a Comparison

Erik Fleischer[a], Wilfried Hofmann[a]

[a] Technische Universiät Dresden, Elektrotechnisches Institut
Helmholtzstraße 9, 01062 Dresden, Germany, erik.fleischer@tu-dresden.de

***Abstract*—This paper analyses a linear and a nonlinear control strategy for a 5-axis magnetic suspension system built with two three pole combined bearings. In these soft magnetic composites (SMC) are used as iron core material to carry the required three-dimensional flux distribution.**

While the linear approach is designed around the CLARKE-Transformation to stabilize the bearing, the nonlinear one is based on feedback linearization to achieve a stable system even in the case of minimal bias flux.

The paper outlines the control strategies and the controller design. Both schemes are compared regarding tracking behavior, decoupling performance and stability margin based on experimental results in the time and frequency domain.

I. INTRODUCTION

Active magnetic bearings have found quite a few applications in vacuum technology especially in high speed machines like turbo molecular pumps. These require bearings which can operate in vacuum. Magnetic bearings are a highly attractive choice in such cases as they do not need any lubricants. Due to the changing magnetization losses are generated in the rotor, which are difficult to dissipate in vacuum.

The three pole combined magnetic bearing has been specifically designed with minimal rotor losses in mind: the pole count has been minimized to three and an axial disc is avoided. Thus it is possible to use mechanically weaker materials like soft magnetic composites (SMC) in the rotor.

Because of the structure there are no distinctive flux path' which can be mapped to the bearing axes like it is typical for conventional bearings. Therefore a different approach to the position control is necessary.

Therefore in this paper two control strategies are outlined and analyzed for a five axis magnetic suspension build using two three pole combined bearings.

Three pole configurations attracted significant attention in the magnetic bearing literature concerning position control strategies. In [1] the CLARKE-Transformation is proposed to map the orthogonal position axes onto the three coil currents and the rotor weight is used to compensate the net force generated by the bias flux.

In [2] an extension to this bearing structure is proposed which adds a homopolar flux path' to generate bias flux with permanent magnets and axial forces. These can be controlled using the zero component in the CLARKE transformation.

Operation without bias usually requires a nonlinear control law. In [3] a surprisingly simple equation is proposed which can be used to calculated the coil currents from a force command in the complex plane. Since such an approach is based on solving for a quadratic root, a systematic algorithm is required to select the best solution [4].

Experimental results report the presence of limiting cycles for both linear and nonlinear approaches in the three pole heteropolar bearing [5]. In [6] a control scheme based on feedback linearization is applied to such a combined bearing with seemingly good results.

II. STRUCTURE OF THE COMBINED THREE POLE BEARING

The main part of the stator consists of three radial poles. Each is wound with one coil as shown in the left part of Fig. 1. This structure is extended by an axial flux path carrying the flux component Φ_a, which is depicted in the cross section view in right part of Fig. 1. Since this flux flows through the rotor frontal area it causes an axial force pulling the rotor along the negative z-direction.

In total there are three control currents, which are sufficient to set three forces in the x-, y- and z-directions. The only limitation exists in the form of a minimum z-axis force, which depends on the actual flux distribution and the forces in x- and y-directions.

A complete five axis suspension requires a second combined bearing flipped around by 180°, which is positioned at the other end of the rotor. Its axial force pulls the rotor in the positive z-direction. In such a structure six currents in total are used to control five degrees of freedom. This means there is

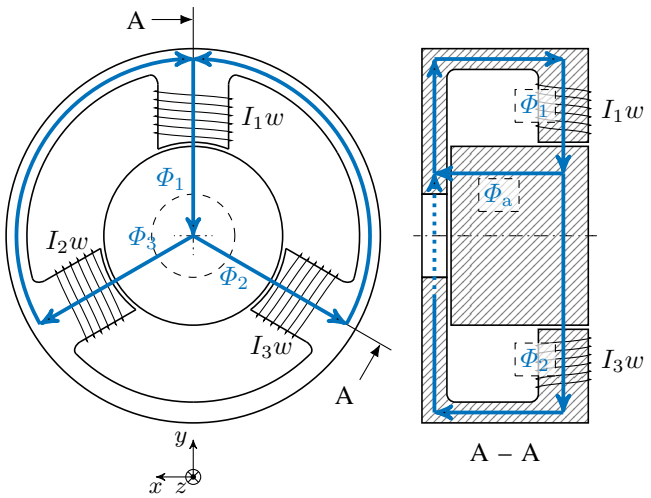

Figure 1. Front and cross section view of the combined bearing with the flux components driven by the current I_1

one current more than necessary, which can be used to either set a bias flux or to minimize the radial flux densities and therefore the rotor losses.

Introducing the axial flux path, one can write for all flux components

$$\Phi_\mathrm{a} = \Phi_1 + \Phi_2 + \Phi_3. \tag{1}$$

Thus sum of the radial flux components Φ_i does not need to be zero. The resulting axial flux component Φ_a can be used for setting the bias flux or for an operation with minimal flux.

Similar to radial flux components the sum of the coil currents is no longer zero as well. A motor inverter consisting of three half bridges is therefore not suitable for operating the bearing.

This structure allows both the rotor and the stator to be build using soft magnetic composites as iron core material. As it can carry a magnetic flux in all directions it is used for all parts. A combination of massive iron parts and laminations can thus be avoided.

III. Control Design

A. Linear Position Control

Based on existing studies two approaches have been chosen for the position control loop. The first one is based on a linear transformation which maps the controller outputs onto the actual coil currents. As the bearing structure employs a pole pitch of 120°, the inverse Clarke transformation can be used as a starting point.

For a complete five axes suspension with two combined three pole bearings this leads to

$$\begin{bmatrix} I_1 \\ I_2 \\ I_3 \\ I_4 \\ I_5 \\ I_6 \end{bmatrix} = \begin{bmatrix} 0 & 1 & & & -1 & 1 \\ \frac{\sqrt{3}}{2} & -\frac{1}{2} & 0 & & -1 & 1 \\ -\frac{\sqrt{3}}{2} & -\frac{1}{2} & & & -1 & 1 \\ & & 0 & 1 & 1 & 1 \\ 0 & & -\frac{\sqrt{3}}{2} & -\frac{1}{2} & 1 & 1 \\ & & \frac{\sqrt{3}}{2} & -\frac{1}{2} & 1 & 1 \end{bmatrix} \begin{bmatrix} I_{\mathrm{x}1} \\ I_{\mathrm{y}1} \\ I_{\mathrm{x}2} \\ I_{\mathrm{y}2} \\ I_\mathrm{z} \\ I_0 \end{bmatrix} \tag{2}$$

$$\boldsymbol{i}_\mathrm{c} = \boldsymbol{T}_\mathrm{i}\, \boldsymbol{i}_{\mathrm{xyz}0} \tag{3}$$

in matrix formulation. The currents I_1 to I_3 represent the coil currents in the bearing on the left end of the rotor, while I_4 to I_6 belong to the bearing on the right end.

The vector $\boldsymbol{i}_{\mathrm{xyz}0}$ contains one control current for each of the five control axes and the bias current I_0. This formulation leads to a quadratic transformation matrix $\boldsymbol{T}_\mathrm{i}$ which can be inverted.

Because of the axial flux path the zero component of the Clarke transformation can be used for axial control and magnetic bias.

Based on previously conducted force measurements [7] it is possible to calculate the force current curves resulting from in the control currents in $\boldsymbol{i}_{\mathrm{xyz}0}$. The results for the radial forces are shown in Fig. 2. The left plot shows the forces in x- and y-directions as a function of I_x. The relationship between I_x and F_x is nearly linear. But there is significant cross coupling resulting in a nonzero $F_\mathrm{y}(I_\mathrm{x})$.

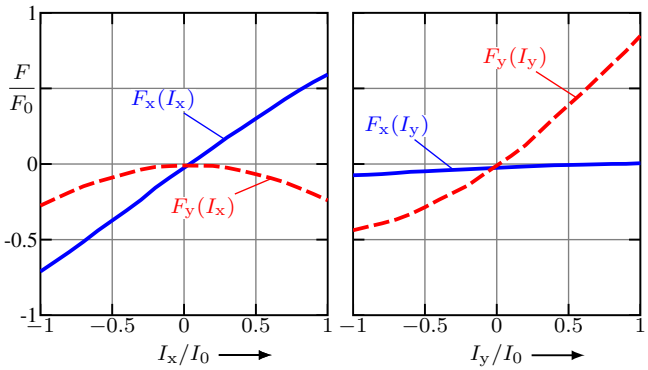

Figure 2. Measured force-current relationship. $I_0 = 2.5\,\mathrm{A}$ and $F_0 = 80.5\,\mathrm{N}$.

The relationship between I_y and F_y in Fig. 2(right) shows some nonlinearity, because the bearing is not symmetric about the x-axis.

The slight cross coupling between I_y and F_x should not occur in theory as there is a symmetry about the y-axis. This distortion is caused by a small excentricity of the rotor during the measurements.

The curves in Fig. 2 show that the control currents can directly be connected to the outputs of five decentral PID controllers. This leads to a reasonable simple control scheme for a magnetic suspension consisting of two combined three pole bearings.

B. Feedback Linearization Control

To deal with the nonlinearity caused by running the bearing with minimal bias flux, an approach based on feedback linearization has been designed [7].

It is based on force commands F_x, F_y and F_z from the position controllers. First F_x and F_y are transformed with

$$F_1 = \begin{cases} 0 & \text{if} \quad F_\mathrm{y} < \dfrac{|F_\mathrm{x}|}{\sqrt{3}} \\ F_\mathrm{y} + \dfrac{|F_\mathrm{x}|}{\sqrt{3}} & \text{else} \end{cases} \tag{4}$$

$$F_2 = F_1 - F_\mathrm{y} + \frac{F_\mathrm{x}}{\sqrt{3}} \tag{5}$$

$$F_3 = F_1 - F_\mathrm{y} - \frac{F_\mathrm{x}}{\sqrt{3}} \tag{6}$$

into the forces F_1, F_2 and F_3 for each pole [8]. From these the radial flux components and thus the currents can be calculated using a magnetic circuit model. Depending on the radial forces there is always an implied force $F_{4\mathrm{imp}}$ along the z-axis in each combined bearing forming a five axis suspension.

The smaller one of these implied forces has to be increased in order to fulfill the force command F_z. This can be done by iteratively solving

$$0 = \pm\sqrt{F_1 + F_0} \pm \sqrt{F_2 + F_0} \pm \sqrt{F_3 + F_0} \pm \sqrt{F_4}k \tag{7}$$

for F_0 where k is the square root of the ratio between the axial and radial air gap cross sections and F_4 the axial force. This equation was derived from (1) by substituting the forces for the flux components and introducing the offset force F_0.

The offset force F_0 is then added to the previously calculated forces F_1, F_2 and F_3 and the result is used to calculate the flux components and the coil currents for the bearing, where the z-axis force has to be increased in order to fulfill the force command F_z.

C. Magnetic Offset Determination

While calculating the currents from the force commands the feedback linearization scheme takes the actual air gap length' into account. These can be calculated from the measured rotor position.

Due to manufacturing tolerances there is usually an offset between the magnetic center of the bearings and the geometrical center of the auxiliary bearings. As in most cases the measurement system is calibrated using the mechanical clearance in the auxiliary bearings, there is an offset in the air gap length' calculated from the measured rotor position.

A significant error can be observed between the force commands necessary for compensating gravity and the expected ones calculated from the rotor weight distribution. Thus the bearing behaves differently from the model used for the controller design. This reduces the stability of the closed control loops and the effectiveness of the decoupling between the x- and y-axes in one bearing.

As these offsets are caused by mechanical tolerances, they have to be determined after the complete assembly and for each unit separately in a series production. For this the observed error between the expected and referenced forces can be utilized. If one measures the currents needed for levitation at multiple rotor positions this error can be calculated. It can be minimized by introducing offsets into the calculation of the air gap length from the measured rotor position. Minimizing this error is a nonlinear optimization problem, which can for example be solved by Powells algorithm [9].

This procedure does not rely on any modifications in the control scheme and can therefore be easily carried out during commissioning of the system after the measurement system has been calibrated.

D. Controller Parameters

The use of Decentral PIDT$_1$ controllers provides the reference commands for both control strategies with the transfer function

$$G_\mathrm{C} = K_\mathrm{p}\left(1 + \frac{1}{T_\mathrm{i}s} + \frac{T_\mathrm{d}}{T_1 s + 1}\right). \tag{8}$$

The used parameters can be found in Table I. For both strategies the same time constants have been used for comparability. The gain has been set for each controller and each axis separately based on the open loop frequency response in such a way that the phase shift is minimal at the cross over frequency, which was set to $50\,\mathrm{Hz}$ in both schemes. This results in a similar closed loop bandwidth in all cases.

The integral part has been set just strong enough to center the rotor with respect to the control axes. The resulting controller gains K_p differ for both control schemes as of the controller output is interpreted differently. Its assumed to be a current in the linear control scheme and a force for the feedback linearization.

Table I
PARAMETERS FOR LINEAR (A) AND FEEDBACK LINEARIZATION (B) CONTROLLERS

	$K_\mathrm{p,x}$	$K_\mathrm{p,y}$	T_i	T_d	T_1
(a)	$0.007\,\frac{\mathrm{A}}{\mu\mathrm{m}}$	$0.007\,\frac{\mathrm{A}}{\mu\mathrm{m}}$	$0.3\,\mathrm{s}$	$3.2\,\mathrm{ms}$	$0.8\,\mathrm{ms}$
(b)	$0.060\,\frac{\mathrm{N}}{\mu\mathrm{m}}$	$0.076\,\frac{\mathrm{N}}{\mu\mathrm{m}}$	$0.3\,\mathrm{s}$	$3.2\,\mathrm{ms}$	$0.8\,\mathrm{ms}$

E. Test Rig

A test rig has been built in which a five axis magnetic suspension using two three pole combined bearings has been realized.

The stators have been constructed using Somaloy Prototyping Material [10] and the active rotor parts using Somaloy 500 LB 1 [11]. Further details on the manufacturing of the bearings can be found in [12]. The main technical specifications have been summarized in Table II.

The rotor has been designed around a steel shaft onto which several rings for an induction machine, the position measurement system and backup bearings have been pressed. In the final manufacturing step massive SMC parts have been glued onto the shaft front faces using Delo Mono Pox 1197 (a single component epoxy glue). The hardening was carried out at $130°$ for $75\,\mathrm{min}$.

The test rig features a horizontal shaft with the y-axis pointing up. Therefore the higher load capacity of the three pole bearings in the direction of a pole can be utilized for compensating gravity.

IV. EXPERIMENTAL COMPARISON

A. Overview

A stable operation of the magnetic suspension has been achieved with the two designed control schemes both with and without taking the magnetic offset described in section III-C into account.

The required currents are summarized in Table III. The results show that with feedback linearization the bearing runs with lower flux densities compared to the linear control scheme. But they are not as low as one would expect from the forces needed to levitate the rotor. Still, the power requirements for the bearing can be reduced to about $30\,\%$.

Table II
TECHNICAL DATA OF THE BEARINGS IN THE TEST RIG

bore diameter	$45\,\mathrm{mm}$
outer diameter	$90\,\mathrm{mm}$
axial length	$40\,\mathrm{mm}$
nominal flux density	$0.8\,\mathrm{T}$
nominal current	$5\,\mathrm{A}$
nominal force	$74.2\,\mathrm{N}$

Table III
MEASURED CURRENTS AND RELATIVE TOTAL OHMIC LOSS P^*_Cu IN THE COILS OF ONE BEARING.

Control Scheme	I_1/A	I_2/A	I_3/A	$P^*_\mathrm{Cu}/\%$
Linear	2.7	2.4	2.5	100
Feedback Linearization	1.9	0.9	0.8	26

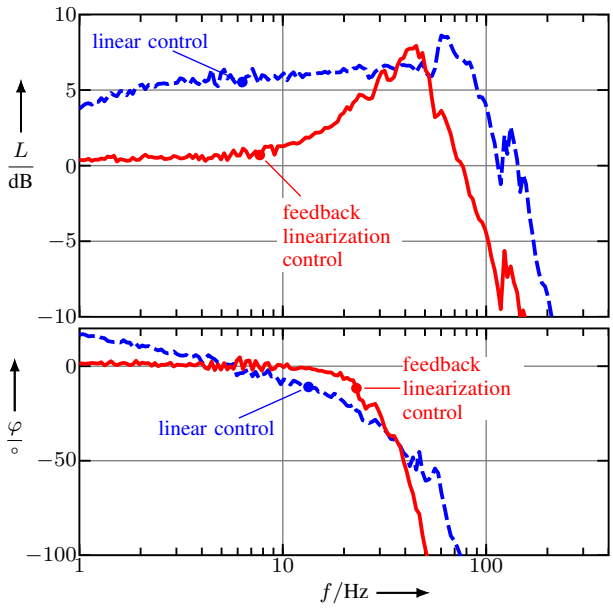

Figure 3. Comparison of closed loop frequency responses of the x_1-axis

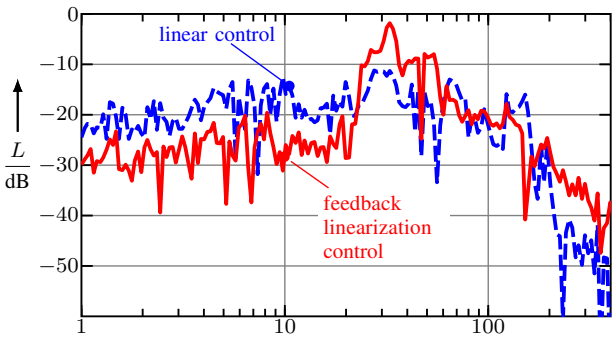

Figure 4. Comparison of cross coupling frequency responses $G = \frac{X_1}{Y_{1\mathrm{ref}}}$

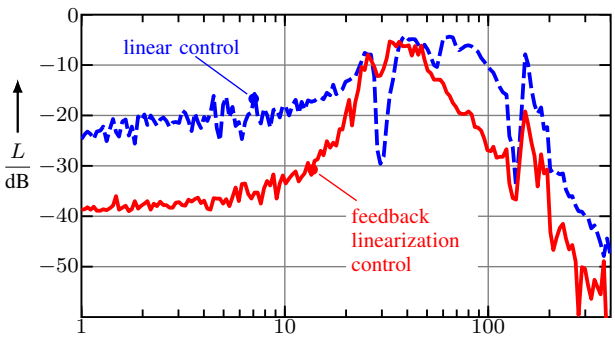

Figure 5. Comparison of cross coupling frequency responses $G = \frac{Y_1}{X_{1\mathrm{ref}}}$

As can be seen from the frequency responses in Fig. 3 both control schemes result in a similar bandwidth with a slightly higher one for the linear scheme. This is mainly due to the biasing, which allows the bearing force to be changed faster.

All measurement have been carried out with the same set of controller parameters found in Table I.

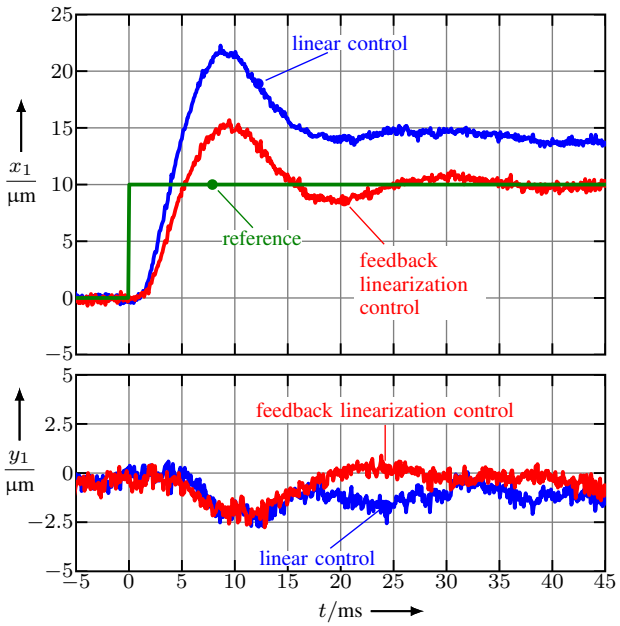

Figure 6. Comparison of step responses along the x_1-axis between linear and feedback linearization control

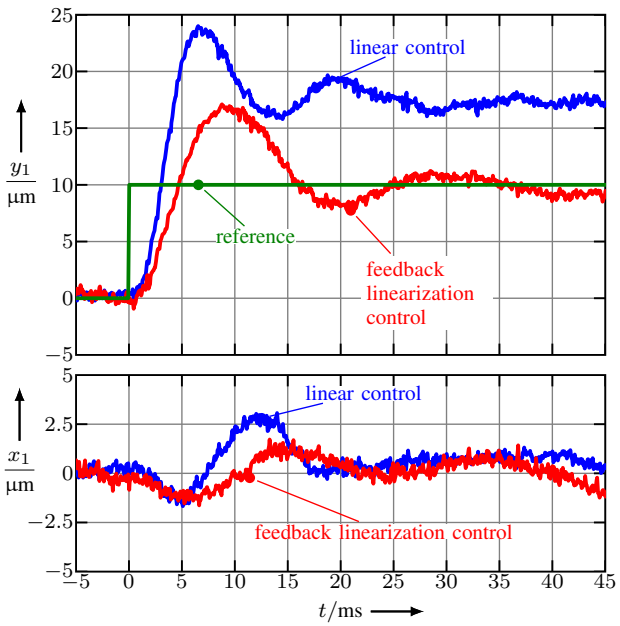

Figure 7. Comparison of step responses along the y_1-axis between linear and feedback linearization control

B. *Impact of the Nonlinear Force-Current Relationship*

Despite the introduction of a bias current in (3) a significant nonlinearity remains in the force-current relationship of the y-axis as shown in Fig. 2 (right). In conjunction with the inherent negative stiffness of the bearing this causes a 4 dB overshoot at frequencies up to 20 Hz as shown in the frequency response in Fig. 3. This indicates a poor tracking behavior, which is confirmed by the step response shown in Fig. 7. It shows a tracking error of 70 % after the initial oscillations have been attenuated. If one compares this result to the step response of the x-axis in Fig. 6, one can see that the overshoot and the

tracking error (40 %) are smaller compared to the y-axis due to the better linearity of the force-current relationship along the x-axis.

As the feedback linearization takes the actual rotor position into account, this effect can be compensated fairly well. The frequency response in Fig. 3 shows a good tracking behavior up to 10 Hz despite the integral part of the PID controller being set to a corner frequency of 0.5 Hz. The step response in Fig. 7 confirms this. The feedback linearization control achieves nearly zero tracking error after the initial overshoot, which is smaller as well.

These results clearly demonstrate that inner loop formed by the feedback linearization can compensate both the static nonlinear behavior and the inherent negative stiffness of the bearings. This leads to good tracking behavior without the need of a strong integral part in the PID controller, which would reduce the stability margin of the control loop.

C. Analysis of Magnetic Cross Coupling Effects

The structure of the three pole bearing magnetically couples all control axes. The following section analyses how well the two schemes are able to decouple the position control loops.

Along the frequency responses of the closed loops the cross coupling has been measured as well. Fig. 4 shows the response of the x_1-axis to changes in the reference value for the y_1-axis in the frequency domain. The analysis in the opposite direction can be found in Fig. 5. Due to the improved tracking behavior the feedback linearization can achieve a better decoupling of the two axes at low frequencies up to 20 Hz. At higher frequencies decoupling behavior becomes similar for both schemes. The impact on the tracking behavior becomes obvious in the step responses.

The lower part of Fig. 6 shows the disturbance of the y-axis while the bearing performs a step on the x-axis on the same plane indicating that the decoupling of the control axes is not complete.

In general there are two possible mechanisms which can cause this effect. The first is that a cross coupling in the feed forward branch remains. Which means a control command along one axis causes a bearing force along another axis as well.

The second mechanism is caused by the position dependence of the magnetic force. That means a movement along one axis requires a change of the control command on another axis in order to keep the magnetic force constant.

Looking at the step response of the x-axis in Fig. 6 one can see that the disturbance on the y-axis is delayed compared to the response of the x-axis which indicates that the disturbance is caused by the position dependence of the magnetic force. As this is not taken into account in the linear control scheme, a tracking error remains.

Until the 15 ms mark the system behaves quite similar with feedback linearization control. After that mark the system actually returns to the reference position. This indicates that the feedback linearization scheme is able to compensate the position dependence of the magnetic force in the steady state. During dynamic processes this compensation does not work as well.

Note that both control schemes employ a very weak integral part in the PID in order to make these effects visible.

The step response of the y-axis shows a different behavior. The disturbance of the x-axis is not delayed indicating a cross coupling in the feed forward control. With both control schemes there is no remaining tracking error after initial oscillation. The main difference is the maximum displacement which is lower with the feedback linearization.

D. Stability Margin

The stability margin is a measure for the damping of oscillations in the system and of the robustness against changes in operating and equipment conditions. One method for evaluating the stability margin, which is also used in ISO 14839-3, is the sensitivity function.

For this analysis the closed loop frequency responses G_c of all control axes of the plant have been measured. From these the open loop frequency responses G_0 can be calculated.

$$G_0 = \frac{G_c}{1 - G_c} \tag{9}$$

The sensitivity function is then defined as in the inverse distance from the critical point (-1, 0).

$$G_S = \frac{1}{1 + G_0} \tag{10}$$

The smallest distance is a measure for the stability margin, which in turn is represented by the maximum of the sensitivity function and is the stability index defined in ISO 14839-3.

The sensitivity function for the y_1-axis has been plotted in Fig. 8. It indicates higher system robustness over wide range of frequencies when operating with feedback linearization control.

For all five control axes the sensitivity function have been calculated and the maximum of each can be found in Table IV. For the two x-axes the values show only small differences.

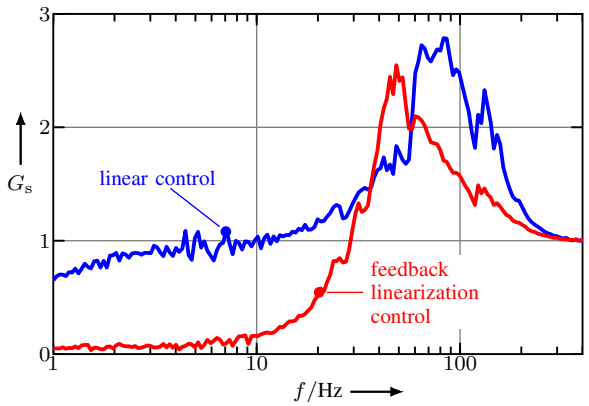

Figure 8. Impact of the control scheme on the sensitivity function of the y_1-axis

Table IV
STABILITY INDICES OF ALL FIVE CONTROL AXES

Axis	x_1	y_1	x_2	y_2	z
Linear Control	2.4	2.8	2.3	2.6	2.6
Feedback Linearization Control	2.4	2.5	2.4	2.5	2.2

This can be attributed to the good linearity of force-current relationship as was shown in Fig. 2. Therefore a similar performance can be expected with both control schemes.

In contrast the curves in Fig. 2 for the y-axes show a remaining nonlinearity in the force-current relationship, which reduces the stability margin of these axes compared to others and feedback linearization scheme. This is especially true for the y_1-axis.

Regarding the z-axis the linear control suffers from the coupling between radial and axial axes as the axial control current I_z acts similar to the bias current I_0 and a change in radial forces always implies an additional axial force in the same bearing.

With the feedback linearization scheme a greater stability margin can therefore be achieved as these cross coupling effects can at least partly be compensated.

It is therefore possible to achieve a similar or slightly better robustness of system with feedback linearization control despite the operation with minimal bias.

V. Conclusion and Outlook

It has been shown that both an approach based on a linear transformation and one based on feedback linearization can stabilize a magnetic suspension which consists of two combined three pole bearings. The stability analysis demonstrated good system robustness with both control schemes.

The comparison has shown that similar or better control performance can be achieved with feedback linearization while operating the bearing at minimal flux densities. Although there were no big gains in decoupling the axes, the tracking behavior can be significantly improved with feedback linearization. The decoupling performances is mainly limited by model accuracy both in terms of the mathematical formulation and the parameters.

Through the operation at minimal currents and flux densities the three pole combined bearing becomes an interesting alternative to permanent magnet bias homopolar bearings. While the copper losses are still somewhat larger, much lower rotor losses are possible.

One of the remaining problems of the feedback linearization scheme is the high computational cost which is mainly due to the ten square root operations for each sampling period of the controller.

Further work on the test rig will concentrate on measuring the rotor losses with different control schemes and comparing the results with conventional bearings.

Acknowledgement

The authors would like to thank the DFG (Deutsche Forschungsgemeinschaft) for funding this project.

References

[1] W. Hofmann, "Behaviour and control of an inverter-fed three-pole active radial magnetic bearing", in *Industrial Electronics, 2003. ISIE '03. 2003 IEEE International Symposium on*, vol. 2, 2003, 974–979 vol. 2.

[2] M. Reisinger, H. Grabner, S. Silber, W. Amrhein, C. Redemann, and P. Jenckel, "A novel design of a five axes active magnetic bearing system", in *12th Intern. Symp. on Mag. Bear.*, 2010.

[3] D. C. Meeker and E. H. Maslen, "Analysis and control of a three pole radial magnetic bearing", in *10th Intern. Symp. on Mag. Bear.*, Citeseer, 2006.

[4] S. Eckhardt and J. Rudolph, "Trajectory tracking for a magnetically levitated shaft with three-phase ambs in y-connection", in *10th Intern. Symp. on Mag. Bear.*, 2006.

[5] S.-L. Chen, Chia-Yi, S.-H. Chen, and S.-T. Yan, "Experimental validation of a current-controlled three-pole magnetic rotor-bearing system", *Magnetics, IEEE Transactions on*, vol. 41, no. 1, pp. 99–112, 2005.

[6] H. Grabner, M. Reisinger, S. Silber, W. Amrhein, C. Redemann, and P. Jenckel, "Nonlinear feedback control of a five axes active magnetic bearing", in *12th Intern. Symp. on Mag. Bear.*, 2010.

[7] E. Fleischer, S. Tröger, and W. Hofmann, "Control of a novel integrated radial-axial magnetic bearing", in *13th Intern. Symp. on Mag. Bear.*, 2012.

[8] S. Eckhardt and J. Rudolph, "High precision synchronous tool path tracking with an amb machine tool spindle", in *9th Intern. Symp. on Mag. Bear.*, 2004.

[9] M. J. D. Powell, "An efficient method for finding the minimum of a function of several variables without calculating derivatives", *The Computer Journal*, vol. 7, no. 2, pp. 155–162, 1964.

[10] Höganäs, *Somaloy technology for electrical motors*, Datenblatt, 2009.

[11] Höganäs, *Somaloy metal powders for smc components*, 2007.

[12] E. Fleischer, S. Tröger, and W. Hofmann, "Development of an active magnetic bearing with a soft magnetic composite core", in *Proceedings of the International Conference Magnetism and Metallurgy*, Jun. 2012.